Organic & Biomolecular Chemistry

ROYAL SOCIETY OF CHEMISTRY

PAPER

View Article Online
View Journal | View Issue

Cite this: *Org. Biomol. Chem.*, 2024, **22**, 1447

DNA nanocrane-based catalysts for region-specific protein modification†

Jordi F. Keijzer and Bauke Albada *

Received 12th December 2023,
Accepted 15th January 2024

DOI: 10.1039/d3ob02025h

rsc.li/obc

This paper describes the development and performance of catalytic DNA-based nanocranes for the controlled modification of wild-type proteins. We show that the position of the catalyst offers control over the region of modification, and that reversible interactions between the catalytic structure and thrombin enable trigger-responsive modification, even in cell lysate.

Introduction

Making chemical changes in the molecular framework of proteins by alteration of the corresponding encoding DNA sequence has resulted in proteins for various specific applications. Due to the density of functional groups on the surface of proteins, controlling post-biosynthesis modification of wild-type or native proteins has only been achieved for a limited set of proteins.[1–5] Although finely-tuned chemical agents and precisely tailored catalytic constructs have yielded approaches that enable the modification of a selective subset of identical functional groups,[2,3,6–9] precise control over modification of native proteins remains challenging, especially within a complex biological setting such as a cell. Our past studies were directed at the development of DNAzymes as enzyme mimics for protein modification,[10–12] the enrichment of thrombin-binding aptamer with catalytic moieties that lead to trigger-responsive site-selective and protein-selective modification,[12] and calibration of the modification efficiency and range with respect to the distance between catalyst and protein.[13] So far, however, it remained to be seen whether complex DNA-based catalytic nanostructures would also be able to selectively modify a protein of interest (POI) in the presence of many other proteins.

In this study, we integrated various elements into novel catalytic structures that (i) reversibly interact with the target protein, (ii) enable control over the protein region that is subjected to modification, and (iii) allow this modification to be performed in the complex mixture of a cell lysate.[8,13–15] To achieve this we use the programmable nature of synthetic DNA to construct various DNA-based nanometer-sized cranes to control modification of native proteins, ideally including external control over the site of the protein that is modified (Fig. 1). We first describe the development of a catalytic tower crane-like nanostructure that reversibly interacts with the metalloprotein carbonic anhydrase 2. Then, we describe two complex DNA-based nanocranes that were designed to control the site of modification by controlling the position of the catalyst on the nanocrane structure. Lastly, we describe the application of those constructs that bind to the protein by means of reversible interactions for the selective modification of thrombin exogenously added to cell lysate.

Results and discussion

Tower crane for modification of carbonic anhydrase 2

Our first strategy to achieve protein modification by means of a reversible interaction was the application of an aromatic sulfonamide as anchor for the DNA construct to the active site of the metalloenzyme carbonic anhydrase 2 (CA2).[16–18] An aromatic sulfonamide binds reversibly to the zinc center in CA2

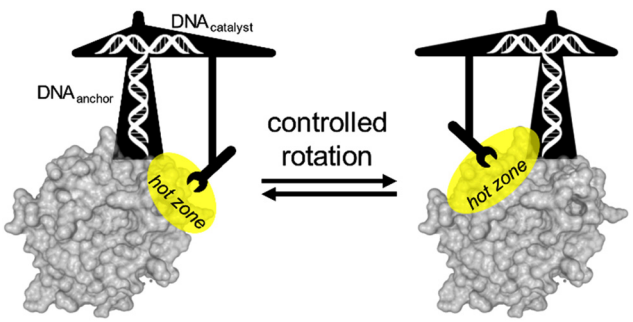

Fig. 1 Schematic depiction of a catalytic DNA-nanocrane for the controlled modification of native proteins. The hot zone indicates the region that is exposed to catalytic protein modification.

Laboratory of Organic Chemistry, Wageningen University & Research, Stippeneng 4, 6708 WE, Wageningen, The Netherlands. E-mail: bauke.albada@wur.nl

†Electronic supplementary information (ESI) available: Synthetic procedures and analytical data, analytical data, details of protein modification experiments. A supplementary video associated to Fig. 3E. See DOI: **https://doi.org/10.1039/d3ob02025h**

by displacing the zinc-bound hydroxyl group in the active site. First, the catalysts, corresponding substrates, and protein anchors were synthesized from commercially available compounds (see Schemes S1–S3, ESI†). In short, alkyne-functionalized DNA strands were clicked by means of CuAAC to the corresponding azide-functionalized protein anchor, to produced DNA_{anchor} strand (Fig. 2A), or catalysts, to produce $DNA_{catalyst}$ strands, of which the most active divalent pyridinium oxime (PyOx) is shown (Fig. 2B, see Scheme S4 and accompanying details in the ESI† for details). Subsequent hybridization of the anchoring DNA (DNA_{anchor}) strand with a catalyst-functionalized DNA ($DNA_{catalyst}$) strand, resulted in the formation of a double-stranded DNA construct designed for the modification of CA2 (Fig. 2C). For this, we tested the configuration where the catalyst was positioned on the same side of the dsDNA helix as the anchor, and formed the dsDNA prior to incubation with CA2.

We used *para*-nitrobenzylamine-*N*-acyl-*N*-sulfonamide as the alkylated *N*-acyl-*N*-sulfonamide (ANANS) substrate for the PyOx-assisted modification of proximal Lys and Ser residues (Fig. 2D).[12,19] We found that the dsDNA construct led to 44% modification of CA2 (DNA : CA2 ratio = 1.9 : 1, pH 7.2), which was significantly higher than the background modification of 6–8% when only the DNA_{diPyOx} strand was present (see Fig. S1, ESI†). Lastly, we pursued CA2-selective modification in *E. coli* cell lysate using a fluorescent lissamine-functionalized ANANS substrate. We found that incorporation of a nitrile instead of the *para*-nitrobenzyl was required to obtain the intended modification (see ESI, section 3.1.6, Fig. S19,† lanes 5–7 and lanes 12–14). Also, CA2 was modified only in the presence of the DNA_{anchor} : DNA_{diPyOx} dsDNA unit, and not when only the DNA_{diPyOx} strand was present (Fig. 2E). As expected, implementing the DMAP-thioester combination did not lead to improved modification (Fig. S20, ESI,† lanes 5–7 and lanes 12–14).[12,19] Due to the observation that the target protein CA2 was only modified when both anchor and catalyst were present, we found evidence that crane-like DNA-based catalytic nanoconstructs can be applied for the modification of proteins in cell lysate.

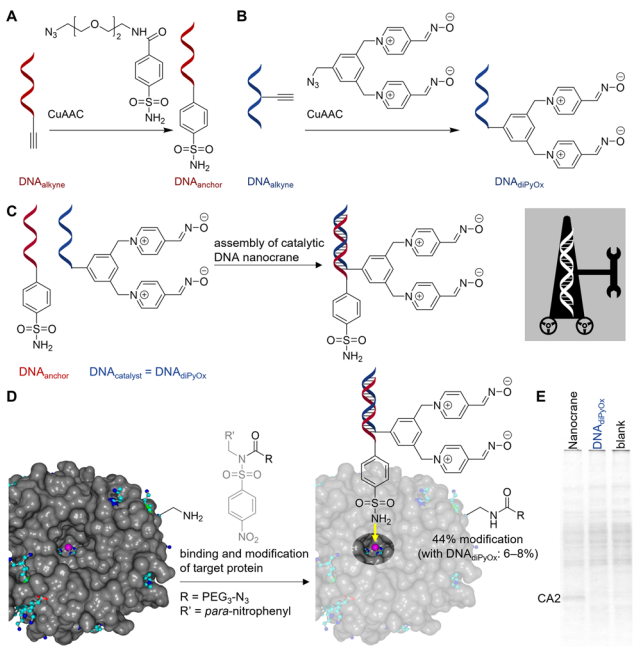

Fig. 2 Chemical modification of carbonic anhydrase 2 (CA2) using a DNA-based nanocrane constructed from DNA_{anchor} and DNA_{diPyOx}. A and B: Synthesis of anchor- and catalyst-functionalized DNA strands. C: Assembly of the DNA-based catalytic nanostructure from an DNA_{anchor} strand that contains the metal-binding sulfonamide and a catalyst-containing DNA_{diPyOx} strand that contains the acylation catalyst. D: Chemical modification of CA2 is more efficient in the presence of the entire DNA nanocrane construct, than when only the catalytic strand is present. E: CA2 modification in *E. coli* cell lysate using nitrile-containing ANANS (R′ = CN) only occurred in the presence of the catalytic DNA nanocrane, even though it was present in the same concentrations in the other two samples (see Fig. S1 in the ESI†).

Following this successful development of a catalytic protein-modifying DNA construct that binds to the target with reversible interactions, we pursued to gain a higher level of control over the site of modification by developing catalytic constructs that would enable differentiation in the positioning of the catalyst with respect to the protein. For this, we tested two designs of the DNA-based catalytic nanostructures that display crane-like features for the modification of human alpha-thrombin: (i) a tower crane-type construct that would enable modification beyond the interface of the two anchor points (Fig. 3A), and (ii) a gantry crane-type design for modification between the anchor points (Fig. 3B).

Tower crane for modification of human alpha-thrombin

The first design that we tested was a tower crane-like construct of which a primary anchor was covalently attached to the active site serine (S195) of thrombin, and a secondary anchor was a non-covalently bound thrombin binding aptamer (Fig. 3A).[20–22] We were particularly interested in a crane-like nanostructure that would enable thrombin modification beyond the region between the two anchors, *i.e.*, on the other side of the protein from the perspective of the secondary anchor. Having access to two thrombin-binding aptamers, TBA and TBA3, which bind to opposite faces of the protein, we would be able to direct the position of the catalyst to two different areas and to assess the ability to control the sites of modification. As can be seen in Fig. 3C, a DNA scaffold ($DNA_{scaffold}$) strand was connected sideways to the active site Ser195 (see Scheme S5, ESI†). One end of this $DNA_{scaffold}$ strand was hybridized to a non-covalent binding DNA_{anchor} strand whereas the other end was functionalized with a variety of $DNA_{catalyst}$ strands having the diPyOx catalyst at different positions. Four different combinations of anchor and catalyst strands were tested: two DNA_{anchor} strands that contained either the TBA or TBA3, and two $DNA_{catalyst}$ strands that contained the diPyOx catalyst[12] at the T6 or at the 5′-end position. For a TBA3-based DNA tower crane that contained the diPyOx catalyst at the 5′-end of the DNA catalyst strand, which positions it at the tip of the tower crane construct, conversions

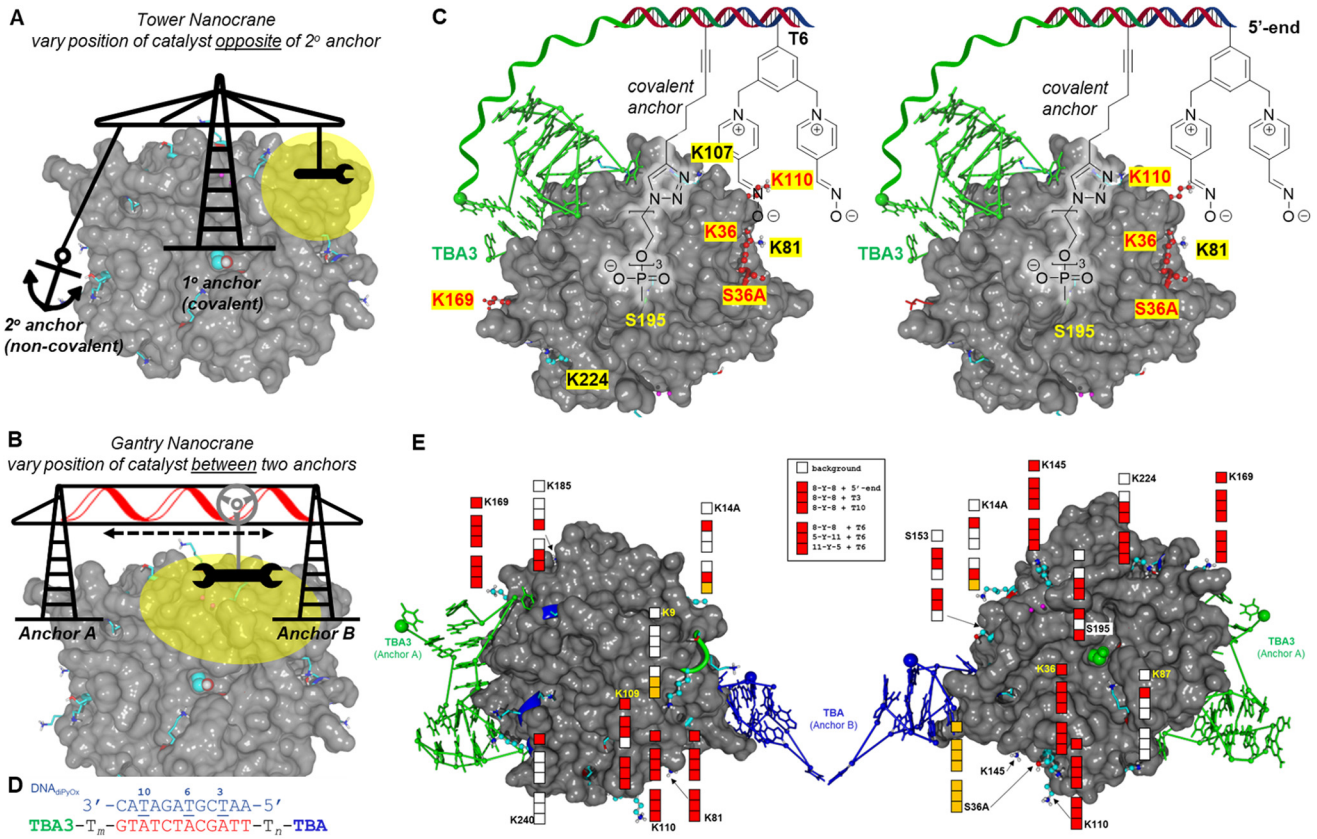

Fig. 3 Development of catalytic DNA nanocranes for the modification of human alpha thrombin (protein is based on the single crystal X-ray structure of human alpha thrombin sandwiched between two aptamers, PDB-code: 5EW2).[20] A and B: Our two DNA nanocrane designs. C: The results of two tower cranes in which a covalent anchor is combined with a non-covalent anchor that directs the site of modification. Modified residues are indicated by the yellow boxes, with residues modified by the DNA_{diPyOx} strand alone in red and residues that are additionally modified by the nanocrane in black. S195 is the active site serine residue that is used for covalent anchoring. D: DNA sequences used for the construction of the gantry crane; the bridge between the two non-covalent aptamer anchors is shown in red, the complementary strand that contains a diPyOx catalyst at the 5′-end or one of the underlined T's is shown in blue. E: Depiction of exposed Lys and Ser residues on two opposite faces of human alpha-thrombin, with the two aptamer anchors that are used to install the DNA_{bridge} to which the DNA_{diPyOx} strand is anchored. Filled boxes indicate which gantry crane led to modification of the corresponding residue (red: >75% localization probability, orange: <75% localization probability, see Table 3). Lys and Ser residues that are not modified are displayed in stick presentation.

were 13–14% for the different designs (see section 3.1.2 in the ESI†).

When the same catalyst was positioned at the T6 position of the $DNA_{catalyst}$ strand, which is closer to the covalent anchor after hybridization to the covalently bound DNA_{anchor} strand, modification efficiencies increased to approximately 27–31% (Fig. S3, ESI†). Analysis of the residues that are modified reveals that the range of modification is extended to modification of K224 (Table 1 and Fig. 3C) (see also section 3.1.3 in the ESI†). In these analyses, localization probability is used to indicate the likelihood that the mentioned residue is modified, a score >90% indicates high probability that this residue has been modified. With the diPyOx catalyst at the 5′-end, modification was restricted to residues on the opposite face of the protein when compared to the position of the non-covalent anchor (Fig. 3C, right). Unfortunately, incorporation of the larger TBA aptamer as secondary anchor did not lead to modification of residues exclusively on the opposite side of the TBA-binding site (Table 1 and Fig. S10, S13, ESI†). Notably, in the absence of the secondary anchor TBA3, the same levels of modification were obtained, indicating that the presence of a

Table 1 Localization probability (%) of modified sites on human alpha-thrombin (TRM) when exposed to different tower crane designs (>90% indicates high probability that this residue has been modified)

	No crane		Tower crane			
Residue	T6	5′	TBA + T6	TBA + 5′	TBA3 + T6	TBA3 + 5′
K36	97	77	84	83	84	83
S36A	50	50	50		50	50
K81	99	99	99	99	99	92
K109			100		100	
K110		100	100	100	100	100
K169	100		99	75	99	76
K186D			100		100	
K224			100		100	
K240		100		100		

second anchor does not improve nor interfere with modification efficiency. Lastly, increasing the spacer length between the second anchor and the dsDNA region of the construct did not improve conversions (Fig. S4, ESI†). Interestingly, application of a triplex-forming oligonucleotide to rigidify the dsDNA structure did not lead to different conversions (Fig. S3, ESI†). Therefore, even though this approach does not yield the same level of modification efficiency than was achieved with the non-covalent binding crane-like construct for carbonic anhydrase 2, we found that the regions of modification are influenced by the design of the catalytic nanocrane.

Gantry crane for the modification of human alpha-thrombin

In order to pursue modification by means of reversible protein binding, we changed our design to a nanocrane that binds to the target protein by means of non-covalent interactions. Specifically, we constructed a DNA-based bridge between two ends of two thrombin-binding aptamers (TBAs, *i.e.*, TBA and TBA3) that bind at opposite faces of thrombin. Hybridization of a variety of catalyst-functionalized $DNA_{catalyst}$ strands to this DNA_{bridge} would result in the formation of a gantry-type crane (Fig. 3B) (see also section 3.1.4 in the ESI†). Using the DNA_{bridge} as an encoded scaffold onto which $DNA_{catalyst}$ strands can be positioned at different points, we were able to test if it would be possible to modify different sites of thrombin by placing the $DNA_{catalyst}$ at different positions (Fig. 3D).

First, we explored the effect of the length of the tether between anchors and bridge on the conversion by inserting thymine-spacers of different length (Table 2, and Fig. S15–S17 in ESI†). As maximum conversions to the modified protein remained low at approximately 15% (our positive control of a TBA_{T12}-diPyOx system typically led to 70–80% modification under the same reaction conditions, see Fig. S4 in the ESI†), we selected three designs for further optimization with the goal of increasing the conversion percentage (*i.e.*, T_8-DNA_{bridge}-T_8, T_5-DNA_{bridge}-T_{11}, and T_{11}-DNA_{bridge}-T_5, Table 2). For this, we prepared different $DNA_{catalyst}$ strands by positioning the catalyst at different positions (*i.e.*, at the 5′-end, T3, T6, or T10, see Fig. 3D) (Fig. S17, ESI†). Screening the position of diPyOx on the $DNA_{catalyst}$ strand revealed highest conversions at either T3 or T6, with conversions of 24% for the T_{11}-DNA_{bridge}-T_5 unit and 21% for the T_8-DNA_{bridge}-T_8 design (Table 2). Despite these low conversions – which could not be improved by implementing the diDMAP-thioester catalyst–substrate combination (see Fig. S18, ESI†) – we determined the residues that were modified by the different cranes (Table 2, ESI†). From this analysis it became clear that both Lys and Ser residues were modified, and that positioning of the catalyst on the bridge exposes residues in different region on thrombin to modification (Fig. 3E).

Not only is a higher number of serine residues modified in the presence of the crane, application of the cranes led to the additional modification of nine lysine residues. Interestingly, exposed lysine residues K60F and K70, which are located in the substrate binding groove are not modified. The fact that Lys240 was not modified in the presence of the crane is attributed to shielding of this residue by TBA3. Lastly, modification of the active site Ser195 was skipped by some of the gantry crane designs. These results indicate that the native reactivity of the residues can be overruled by the nanocranes.

Switchable protein modification in cell lysate

Following the successful application of the CA2-modifying nanocrane in *E. coli* cell lysate, we tested the most-active DNA gantry-type nanocrane for the modification of thrombin (*i.e.*, T_8-DNA_{bridge}-T_8/T6, abbreviated as '8Y8/T6' in Fig. 4). As reference, we applied an earlier aptamer-diPyOx construct (TBA_{T12}-diPyOx), which would also be applicable for *in situ* switching

Table 2 Conversion percentages associated to the various gantry cranes that were used after 5 h incubation with the ANANS 2 substrate

T-tether			Catalyst strand		
m	*n*	5′-End	T3	T6	T10
No DNA crane		2		1	
5	5	5		14	
6	6	9		16	
7	7	8		17	
3	11	4		12	
11	3	9		13	
8	8	9	11	21	11
5	11	5	19	21	6
11	5	13	14	24	11
9	9	9		9	
6	12	6		12	
12	6	10		14	

Table 3 Localization probability (%) of modified sites on human alpha-thrombin (TRM) when exposed to a gantry crane that carries the diPyOx catalyst at different positions (>90% indicates high probability that this residue has been modified). Residues modified by only the 5′-end DNA_{diPyOx} strand are indicated by the asterisk (*); the one-letter code for the active site Ser195 is depicted in bold

	Catalyst position			Gantry sequence		
				T6		
Position diPyOx:	5′	T3	T10			
Gantry design:	T_8YT_8	T_8YT_8	T_8YT_8	T_8YT_8	T_5YT_{11}	$T_{11}YT_5$
Residue						
K9					50	50
K14A	99				99	50
K36*	96	98	97	99	100	91
S36A*	50		50	50	50	50
K81	100	100	100	100	99	100
K87	100					
K109	100	100		98	96	99
K110*	100	100	100	100	100	100
K135	61	61	61	61		
K145*	100	100	100	100	100	100
S153	100	100		100	100	
K169*	98	84	100	83	77	99
K185			100		95	100
K186D	100	100	100	100	100	100
S195		100	100	100		100
K224		100	100	100	100	100
K240*						

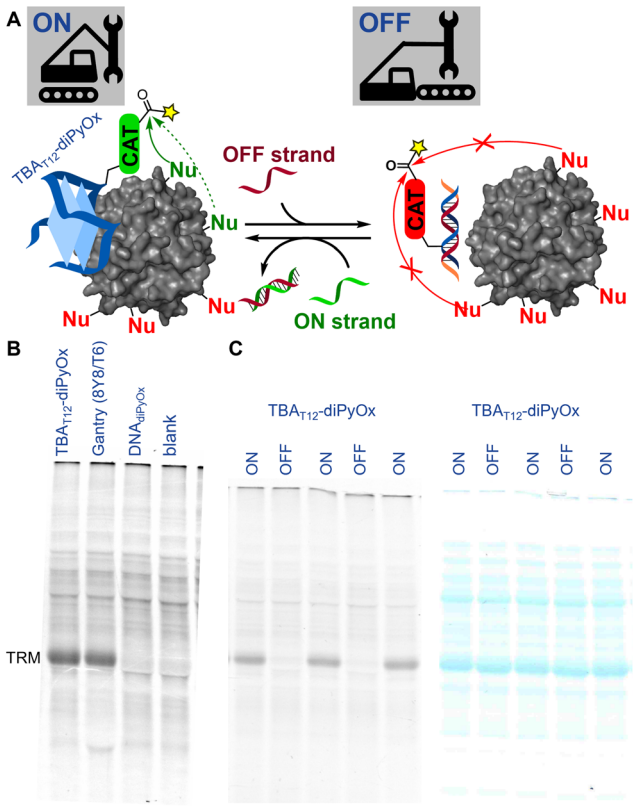

Fig. 4 Thrombin-selective modification by DNA-based catalytic nanostructures in *E. coli* cell lysate (TRM = thrombin; it was present in all samples run in all lanes). A: Schematic depiction of the ON–OFF switchable thrombin modification by means of an excavator-type TBA$_{T12}$-diPyOx construct and a pair of orthogonally complementary strands.[12] B: Fluorescence image of a gel that indicates thrombin-selective modification by gantry nanocrane T$_8$-DNA$_{bridge}$-T$_8$/T6, abbreviated as 8Y8/T6, is on the same level as that of TBA$_{T12}$-diPyOx,[12] the DNA$_{diPyOx}$ strand alone does not lead to modification above background. C: Left: fluorescence image of a gel that indicates switching of the activity of the excavator-type TBA$_{T12}$-diPyOx nanostructure in cell lysate controls thrombin-selective modification. Right: Coomassie stain shows similar levels of all proteins are present in the mixtures.

(Fig. 4A).[12,23] Even though the gantry nanocrane relies on the hybridization of two DNA strands to form the active construct, we found that thrombin-selective modification by the gantry nanocrane was on the same level as that of the single-stranded TBA$_{T12}$-diPyOx construct (Fig. 4B, lanes 1 and 2). In the absence of the gantry DNA, modification of thrombin was not detected (Fig. 4B, lane 3). Despite the relatively low modification efficiency of the gantry crane on the isolated protein, its performance in cell lysate was as good as that of our best-performing construct (*cf.* lanes 1 and 2 and Fig. 4B). To assess switchable protein modification in cell lysate, we focused on the diPyOx catalyst-functionalized thrombin-binding aptamer TBA$_{T12}$-diPyOx construct that was disclosed earlier.[12] Fortunately, we were able to switch the modification activity of the excavator-type construct TBA$_{T12}$-diPyOx ON and OFF repeatedly, even in *E. coli* cell lysate (Fig. 4C).

Conclusions

In conclusion, we describe the development of novel DNA-based crane-like nanoconstructs for protein modification. We showed that DNA-based nanocranes can use either one or two non-covalent protein anchors, or a combination of a covalent and non-covalent protein anchor, to perform chemical protein modification. Although modest conversions and primitive levels of control over the sites of modification have been obtained, it can be expected that a higher level of control over the nanocrane structure and components will lead to improvement of both aspects. For example, we expect that this can be obtained by reducing the length of the spacer between the DNA core and anchor or catalyst, or both, significantly below the current 19 atoms that are minimally present between DNA scaffold and the anchor or catalyst. Nevertheless, protein-selective modification in *E. coli* cell lysate was achieved by the gantry nanocrane, and switchable modification was shown using an aptamer-catalyst construct. As such, this study shows the development of complex DNA-based nanocrane-like structures for controlled protein modification, even in the complex biological mixture of a cell lysate. Although ON/OFF-switchable activity of the DNA-based nanocranes in cell lysate was not proven yet, the fact that this was possible for the single-stranded DNA-based excavator-type construct proves that such a feature can be installed in catalytic protein modifying DNA nanostructures.

Conflicts of interest

There are no conflicts to declare.

Acknowledgements

We thank Mangala Srinivas and Navya Nayak (Cell Biology & Immunology, Wageningen University & Research, the Netherlands) for providing us with the *E. coli* cell lysates. We thank the Wageningen University & Research for funding.

References

1 J. J. Bruins, D. Blanco-Ania, V. Van Der Doef, F. L. Van Delft and B. Albada, *Chem. Commun.*, 2018, **54**, 7338–7341.
2 E. A. Hoyt, P. M. S. D. Cal, B. L. Oliveira and G. J. L. Bernardes, *Nat. Rev. Chem.*, 2019, **3**, 147–171.
3 B. Albada, J. F. Keijzer, H. Zuilhof and F. van Delft, *Chem. Rev.*, 2021, **121**, 7032–7058.
4 O. Boutureira and G. J. L. Bernardes, *Chem. Rev.*, 2015, **115**, 2174–2195.
5 J. Kalia and R. T. Raines, *Curr. Org. Chem.*, 2010, **14**, 138–147.
6 N. C. Reddy, M. Kumar, R. Molla and V. Rai, *Org. Biomol. Chem.*, 2020, **18**, 4669–4691.
7 J. F. Keijzer and B. Albada, *Biopolymers*, 2021, **113**, 1–8.

8 B. Albada, *ChemBioChem*, 2023, **24**, 1–5.
9 S. K. Silverman, *Acc. Chem. Res.*, 2015, **48**, 1369–1379.
10 J. F. Keijzer and B. Albada, *Bioconjugate Chem.*, 2020, **31**, 2283–2287.
11 S. Wintermans, J. F. Keijzer, M. Dros, H. Zuilhof and B. Albada, *ChemCatChem*, 2021, **13**, 4618–4624.
12 J. F. Keijzer, J. Firet and B. Albada, *Chem. Commun.*, 2021, **57**, 12960–12963.
13 J. F. Keijzer, H. Zuilhof and B. Albada, *Chem. – Eur. J.*, 2022, **28**, 1–8.
14 Y. Biniuri, B. Albada, M. Wolff, E. Golub, D. Gelman and I. Willner, *ACS Catal.*, 2018, **8**, 1802–1809.
15 K. Shiraiwa, R. Cheng, H. Nonaka, T. Tamura and I. Hamachi, *Cell Chem. Biol.*, 2020, **27**, 970–985.
16 J. Y. Winum, S. A. Poulsen and C. T. Supuran, *Med. Res. Rev.*, 2009, **29**, 419–435.
17 M. Aggarwal, B. Kondeti and R. McKenna, *Bioorg. Med. Chem.*, 2013, **21**, 1526–1533.
18 P. Zhao, Z. Chen, Y. Li, D. Sun, Y. Gao, Y. Huang and X. Li, *Angew. Chem., Int. Ed.*, 2014, **53**, 10056–10059.
19 S. Tsukiji, M. Miyagawa, Y. Takaoka, T. Tamura and I. Hamachi, *Nat. Chem. Biol.*, 2009, **5**, 341–343.
20 I. R. Krauss, A. Merlino, A. Randazzo, E. Novellino, L. Mazzarella and F. Sica, *Nucleic Acids Res.*, 2012, **40**, 8119–8128.
21 D. M. Tasset, M. F. Kubik and W. Steiner, *J. Mol. Biol.*, 1997, **272**, 688–698.
22 A. Pica, I. R. Krauss, V. Parente, H. Tateishi-Karimata, S. Nagatoishi, K. Tsumoto, N. Sugimoto and F. Sica, *Nucleic Acids Res.*, 2017, **45**, 461–469.
23 F. Wang, X. Liu and I. Willner, *Angew. Chem., Int. Ed.*, 2015, **54**, 1098–1129.